A CHEBYSHEV COLLOCATION SPECTRAL METHOD FOR NUMERICAL SIMULATION OF INCOMPRESSIBLE FLOW PROBLEMS

Johnny J. Martínez R
Department of Ocean Engineering, Federal University of Rio de Janeiro,
EE-COPPE/UFRJ, CP68.508; 21945-970 Rio de Janeiro, RJ, Brazil
Martinez@peno.coppe.ufrj.br

Paulo T.T. Esperança
Department of Ocean Engineering, Federal University of Rio de Janeiro,
EE-COPPE/UFRJ, CP68.508; 21945-970 Rio de Janeiro, RJ, Brazil
ptarso@peno.coppe.ufrj.br

Abstract. This paper concerns with the numerical simulation of internal recirculating flows, of a two-dimensional viscous incompressible flow generated inside a regularized square driven cavity and over a backward-facing step. For this purpose, the simulation is performed by using the projection method combined with a Chebyshev collocation spectral method. The incompressible Navier-Stokes equations are formulated in terms of the primitive variables, velocity and pressure. The time integration of the spectrally discretized, incompressible Navier-Stokes equations is performed by a second-order mixed explicit/implicit time integration scheme. This scheme is a combination of the Crank-Nicolson scheme operating on the diffusive term and Adams-Bashforth scheme acting on the advective term. The projection method is used to split the solution of the incompressible Navier-Stokes equations to the solution of two decoupled problems: the Burgers equation to predict an intermediate velocity field and the Poisson equation for the pressure, that is used to correct the intermediate velocity field and satisfy the continuity equation. Numerical simulations for flows inside a two-dimensional regularized square driven cavity for Reynolds numbers up to 10000 and over a backward-facing step for Reynolds numbers up to 875 are presented and compared with numerical results previously published, where good agreement is demonstrated.

Keywords. Chebyshev collocation method, Incompressible Navier-Stokes equations, Projection method, Crank-Nicolson scheme, Adams-Bashforth scheme.

1. Introduction

The main objective of this current work is to develop an efficient numerical method of solution for two dimensional viscous incompressible flow with internal recirculating flows generated inside of a regularized square driven cavity and over a backward-facing step. For this purpose, the numerical simulation of incompressible Navier-Stokes equations in two dimensions (INSE2D) is based upon a Chebyshev collocation spectral method (also named Chebyshev pseudospectral method) in conjunction with a projection method. The motivation for the use of collocation spectral methods stems from their high precision, as well as their very low phase errors for the prediction of time-dependent flow regimes. A time integration of the equations system is performed with a semi-implicit second-order accurate scheme (Adams-Bashforth and Crank-Nicolson).

One major problem in solving incompressible Navier-Stokes equations comes from the coupling of the pressure with the velocity, to satisfy the incompressibility condition. Different methods were proposed to overcome this difficulty. The use of vorticity and streamfunction formulation of the equations avoids this problem. However, although its application to two-dimensional flows is common, its extension to three-dimensional problems is not straightforward. Thus, the primitive variable formulation is found to be most easily extended to 3-D flows. For this type of formulation, Chorin (1968) and Temam (1968) proposed the projection method (or fractional step method) to overcome the lack of evolution equation for the pressure in this formulation, which is known to be a source of difficulty.

The paper is organized as follows. In section 2, is presented the mathematical formulation, including the governing equations and the projection method. The section 3, is devoted to the numerical formulation, consisting of the spatial discretization and the solution method. For last, in section 4 the numerical results of the two-dimensional regularized driven square cavity flow for Reynolds numbers of 100 up to 10000 and flows over a backward-facing step for Reynolds numbers up to 875 are presented and compared with numerical results previously published.

2. Mathematical formulation

2.1. Governing Equations

Two-dimensional viscous incompressible fluid flows are governed by the Navier-Stokes equations. The dimensionless unsteady Navier-Stokes equations for incompressible flows in Cartesian coordinates may be written in primitive variables as

$$\frac{\partial V}{\partial t} + (V.\nabla)V = -\nabla P + \frac{1}{Re}\nabla^2 V \qquad \text{in } \Omega . \qquad (1)$$

$$\nabla . V = 0 \qquad\qquad \text{in } \Omega \qquad\qquad (2)$$

where the unknowns are the vector $V = (u,v)^T$, which represents the velocity of the flow, and the scalar P, which represents the pressure field. Here, $\mathbf{Re}$ is the Reynolds number of the flow $\left(\mathbf{Re} = U_o L_c / \upsilon\right)$, U_o is the free-stream velocity, L_c represents the characteristic length and υ the kinematic viscosity. Let Ω be the internal computational domain with sufficiently smooth boundaries $\partial\Omega$. The initial condition is given as

$$V\big|_{t=0} = w_o \qquad\qquad \text{in } \Omega . \qquad\qquad (3)$$

satisfying Eq. (2), is important that this initial velocity field be divergence free otherwise the continuous problem does not possess a classical solution. The Eqs. (1) and (2) are completed with an appropriate boundary condition for the velocity field, such that:

$$V = w \qquad\qquad \text{on } \partial\Omega . \qquad\qquad (4)$$

The Navier-Stokes equations were non-dimensionalized using the following dimensionless variables:

$$x' = \frac{x}{L_c}, \ y' = \frac{y}{L_c}, \ t' = \frac{tU_\infty}{L_c}, \ P' = \frac{P}{\rho U_\infty^2}, \ V' = \frac{V}{U_\infty}$$

2.2. Projection method

A major difficulty to solve numerically the incompressible Navier-Stokes equations (INSE) comes from that the velocity V and the pressure P are coupled together by the incompressibility constraint $\nabla . V = 0$. To overcome this difficulty, Chorin (1968) and Temam (1968), proposed the projection method (or fractional step method), which decouples the velocity and the pressure fields. The projection method has been widely used and has proven to be very efficient for this type of problem.

These classes of methods permit uncouple the velocity and the pressure in each time step by reducing the solution of the Navier-Stokes equations to the solution of two successive problems. The first step solves an intermediate velocity, which does not satisfy the incompressibility condition (the velocity field is not solenoidal), while in the second step the intermediate velocity is projected onto a divergence-free space. This last step is equivalent to the solution of a Poisson equation for pressure, which is used to correct the intermediate velocity in order to fulfill the incompressibility condition.

The projection methods are based on the observation that the left-hand side of Eq. (1) is a Hodge decomposition. Hence an equivalent projection scheme is given by

$$\frac{\partial V}{\partial t} = \wp\left[-(V.\nabla)V + \frac{1}{\mathbf{Re}}\nabla^2 V\right]. \qquad\qquad (5)$$

where $\wp$ is the operator which projects a vector field onto the space of divergence-free vector fields with appropriate boundary conditions.

The projection $\wp$ can be defined by the solution of a Poisson equation. Specifically, let $W = V + \nabla\phi$ be the Hodge decomposition of W, where ϕ is a scalar field and V is divergence-free velocity field that is required to satisfy $V\big|_{\partial\Omega} = w$. Then to determine V from W let (Brown et al. (2001))

$$V = \wp(W) = W - \nabla\phi . \qquad\qquad (6)$$

where

$$\nabla^2\phi = \nabla . W \qquad\qquad \text{in } \Omega , \qquad\qquad (7)$$

$$\hat{n}.\nabla\phi = \hat{n}.(W - w) \qquad\qquad \text{on } \partial\Omega . \qquad\qquad (8)$$

Following Streett & Macaraeg (1989/90), the semi-discretized version of a semi-implicit projection method can be written in two steps as follows:

a.. The advection-diffusion step solves the intermediate velocity field $\widetilde{V}$ by

$$\frac{\widetilde{V} - V^n}{\Delta t} = \frac{1}{Re} \nabla^2 \widetilde{V} - (V^n . \nabla) V^n \qquad \text{in } \Omega \text{ ,} \qquad (9)$$

with the intermediate boundary conditions

$$\hat{\tau} . \widetilde{V} = \hat{\tau} . V + \hat{\tau} . \Delta t (2 \nabla P^n - \nabla P^{n-1}) \qquad \text{on } \partial \Omega \text{ ,} \qquad (10)$$

$$\hat{n} . \widetilde{V} = \hat{n} . V \qquad \text{on } \partial \Omega \text{ .} \qquad (11)$$

b. The pressure correction step solves the Poisson equation for P from

$$\nabla^2 P^{n+1} = \frac{\nabla . \widetilde{V}}{\Delta t} \qquad \text{in } \Omega \text{ ,} \qquad (12)$$

with the boundary condition:

$$\hat{n} . \nabla P^{n+1} = 0 \qquad \text{on } \partial \Omega \text{ .} \qquad (13)$$

Then the velocities are updated with

$$V^{n+1} = \widetilde{V} - \Delta t . \nabla P^{n+1} \qquad \text{in } \Omega + \partial \Omega \text{ .} \qquad (14)$$

In summary, this step can be viewed as the projection of the velocity field onto the divergence-free space.

3. Numerical formulation

3.1. Spatial discretization

The Equations (9) and (12) obtained of the semi-discretized version of the projection method are spatially discretized using a Chebyshev collocation spectral method. All the dependent variables u, v, P are expanded in double truncated series of Chebyshev polynomials. The collocation spectral method is characterized by the fact that the solution discretized is forced to satisfy the governing equations only at collocation points. So, the series expansion for a function $u(x)$ may be approximated as

$$u_N(x) = \sum_{k=0}^{N} \hat{u}_k \, \phi_k(x) , \qquad (15)$$

where the $\phi_k(x)$ are the basis functions and the $\hat{u}_k$ are the expansion coefficients. For a Chebyshev collocation scheme, the functions $\phi_k(x) = T_k(x) = \cos(k \cos^{-1} x)$ are the Chebyshev polynomials and the interpolation points are the called Chebyshev-Gauss-Lobatto points

$$x_i = \cos\left(\frac{\pi i}{N}\right). \qquad i = 0, 1,..., N \text{ .} \qquad (16)$$

The expansion coefficients, $\hat{u}_k$ may be evaluated by the inverse relation

$$\hat{u}_k = \frac{2}{N c_k} \sum_{i=0}^{N} \frac{u_i}{c_i} \cos\left(\frac{k \pi i}{N}\right), \qquad k = 0, 1,..., N \text{ .} \qquad (17)$$

where c_i and $c_k = 1$ for $i, k = 1, 2,.., N-1$ and $c_0 = c_N = 2$.

The differentiation can be accomplished in transform space (named transform method) or in physical space (matrix multiplication method). The first method can be performed efficiently by means of a fast cosine transform with a recurrence relation in spectral space (see Canuto et al. (1988)) and second method is based in explicit expressions

obtained by differentiating the Lagrange polynomials. The matrix multiplication method is used in this paper because is very efficient and easy to implement.

The derivative of $u_N(x)$ at the collocation points x_i is estimated by the analytical derivative of the Lagrange polynomials evaluating it at the collocation points x_i,

$$u'_N(x_i) = \sum_{k=0}^{N} D_{ik}^{(1)} u_k \,, \tag{18}$$

where $D^{(1)}$ is the Chebyshev collocation derivative matrix. This matrix $D^{(1)}$ is given by (Canuto et al. (1988))

$$D_{ik}^{(1)} = \begin{cases} \dfrac{c_i\,(-1)^{i+k}}{c_k(x_i - x_k)}, & i \neq k, \\[2ex] -\dfrac{x_k}{2\,(1 - x_k^2)}, & 1 \leq i = k \leq N\text{-}1, \\[2ex] \dfrac{2N^2 + 1}{6}, & i = k = 0, \\[2ex] -\dfrac{2N^2 + 1}{6}, & i = k = N. \end{cases} \tag{19}$$

The second collocation derivative matrix $D^{(2)}$ can be computed analytically or by the following relation $D^{(2)} = (D^{(1)})^2$, (Boyd (2001)).

3.2. Temporal discretization

The temporal integration is based on a second-order explicit-implicit scheme, which combines an explicit second-order Adams-Bashforth scheme for the advection terms and an implicit Crank-Nicolson scheme for treats the viscous terms.

The Burgers and Poisson equations obtained of the projection method are solved by using a complete diagonalization of the operators in both directions, (Chen et al. (2000)). The computation of eigenvalues, eigenvectors and the inversion of the corresponding matrices are done once in a preprocessing step before starting the time integration. Thus, at each time step iteration, the solution is obtained from simple matrices products.

4. Numerical results

4.1. Regularized square driven cavity flow

The regularized square driven cavity (see Fig. (1a)) is a model for flow in a cavity where the upper boundary moves to the right with a horizontal velocity distribution of $16x^2(1 - x)^2$, while the other three boundaries are kept stationary (no-slip boundary conditions) and this generate the internal recirculating flow in the cavity. The initial condition for all cases, starts from rest.
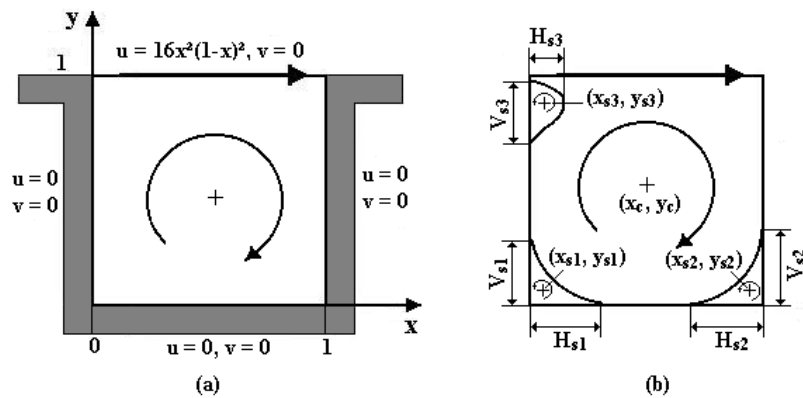
Figure 1. Regularized square driven cavity flow: (a) Boundary conditions; (b) Flow configuration and nomenclature (Tanahashi et al. (1990))

The flow configuration is characterized by the magnitude and the location of the centers of the primary and secondary vortices. The Tab. (1) shows the comparison of the some characteristic values of the regularized square driven cavity flow with previous numerical results obtained by Shen (1991), according to the nomenclature in Fig. (1b). Shen (1991) used the projection scheme of Kim & Moin (1985) in conjunction with a Chebyshev-Tau space discretization. The Shen (1991) results were based on uniform grids of 17x17 up to 49x49 depending of the Reynolds numbers (see Tab. (1)). Although we have used only a 33x33 mesh for all cases, the solutions are in good agreement with theirs.

Table 1. Comparison of some characteristic values of the stream functions

Re	Parameter	Present Method	Shen (1991)
100 (17x17)	(x_c,y_c) (x_{s1},y_{s1}) (x_{s2},y_{s2}) $(H_{s1}, V_{s1});(H_{s2},V_{s2})$	(0.607, 0.753) (0.032, 0.032) (0.955, 0.052) (0.13, 0.14);(0.14, 0.14)	(0.609, 0.750) (0.031, 0.031) (0.953, 0.047)
400 (17x17)	(x_c,y_c) (x_{s1},y_{s1}) (x_{s2},y_{s2}) $(H_{s1},V_{s1});(H_{s2},V_{s2})$	(0.578, 0.615) (0.045, 0.041) (0.900, 0.115) (0.135, 0.110);(0.250, 0.315)	(0.578, 0.625) (0.031, 0.047) (0.922, 0.094)
1000 (25x25)	(x_c,y_c) (x_{s1},y_{s1}) (x_{s2},y_{s2}) $(H_{s1},V_{s1});(H_{s2},V_{s2})$	(0.545, 0.575) (0.077, 0.068) (0.876, 0.118) (0.205, 0.170);(0.320, 0.335)	(0.547, 0.578) (0.078, 0.063) (0.922, 0.094)
2000 (33x33)	(x_c,y_c) (x_{s1},y_{s1}) (x_{s2},y_{s2}) (x_{s3},y_{s3}) (H_{s1},V_{s1}) $(H_{s2},V_{s2});(H_{s3},V_{s3})$	(0.535, 0.555) (0.09, 0.09) (0.856, 0.107) (0.028, 0.888) (0.255, 0.195) (0.35, 0.35);(0.05, 0.14)	(0.531, 0.547) (0.094, 0.094) (0.922, 0.094) (0.031, 0.908)
5000 (33x33)	(x_c,y_c) (x_{s1},y_{s1}) (x_{s2},y_{s2}) (x_{s3},y_{s3}) (H_{s1},V_{s1}) $(H_{s2},V_{s2});(H_{s3},V_{s3})$	(0.518, 0.543) (0.081, 0.121) (0.818, 0.081) (0.082, 0910) (0.350, 0.270) (0.370, 0.415);(0.130, 0.260)	(0.516, 0.531) (0.094, 0.094) (0.922, 0.094) (0.078, 0.908)
10000 (49x49)	(x_c,y_c) (x_{s1},y_{s1}) (x_{s2},y_{s2}) (x_{s3},y_{s3}) (H_{s1},V_{s1}) $(H_{s2},V_{s2});(H_{s3},V_{s3})$	(0.509, 0.523) (0.080, 0.140) (0.772, 0.063) (0.090, 0.915) (0.350, 0.300) (0.390, 0.440);(0.173, 0.315)	(0.516, 0.531) (0.094, 0.094) (0.922, 0.094) (0.094, 0.908)

The Figs. (2c)-(2f) show the streamlines of the steady state of the regularized square driven cavity flow for Reynolds numbers up to 10000. In these figures can be noted the variation of the magnitude and location of the centers of the primary and secondary vortices with Reynolds numbers.

In the Figs. (2a), (2b) and (2c) can also be observed the formation and growing of the secondary vortices at the bottom left and bottom right of the cavity when the Reynolds number increases. These figures show mainly that the secondary vortices for the Reynolds numbers studied can be very well represented using only 33x33 points of collocation, thanks to the condensed distribution of the Chebyshev-Gauss-Lobatto points near the boundary.

The Figs. (2d), (2e) and (2f) show the streamlines contours of the steady flow for three Reynolds numbers (Re = 2000, 5000 and 10000). Once again, can be observed the formation, evolution and growing of other secondary vortex than appears at the top left of the regularized cavity. At Re = 10000, a tertiary vortex becomes visible at the bottom right of the cavity with the center in (0.945,0.04) and another tertiary vortex begins to appear at the top right corner.

Once more, these figures show than the secondary and tertiary vortices for Reynolds numbers up 10000 can be very well represented with only 33x33 points of collocation.

Finally, the variation of the u and v velocity profiles on the centerlines of the regularized driven cavity for Reynolds numbers up to 10000 are shown in the Fig. (3a) and Fig.(3b).
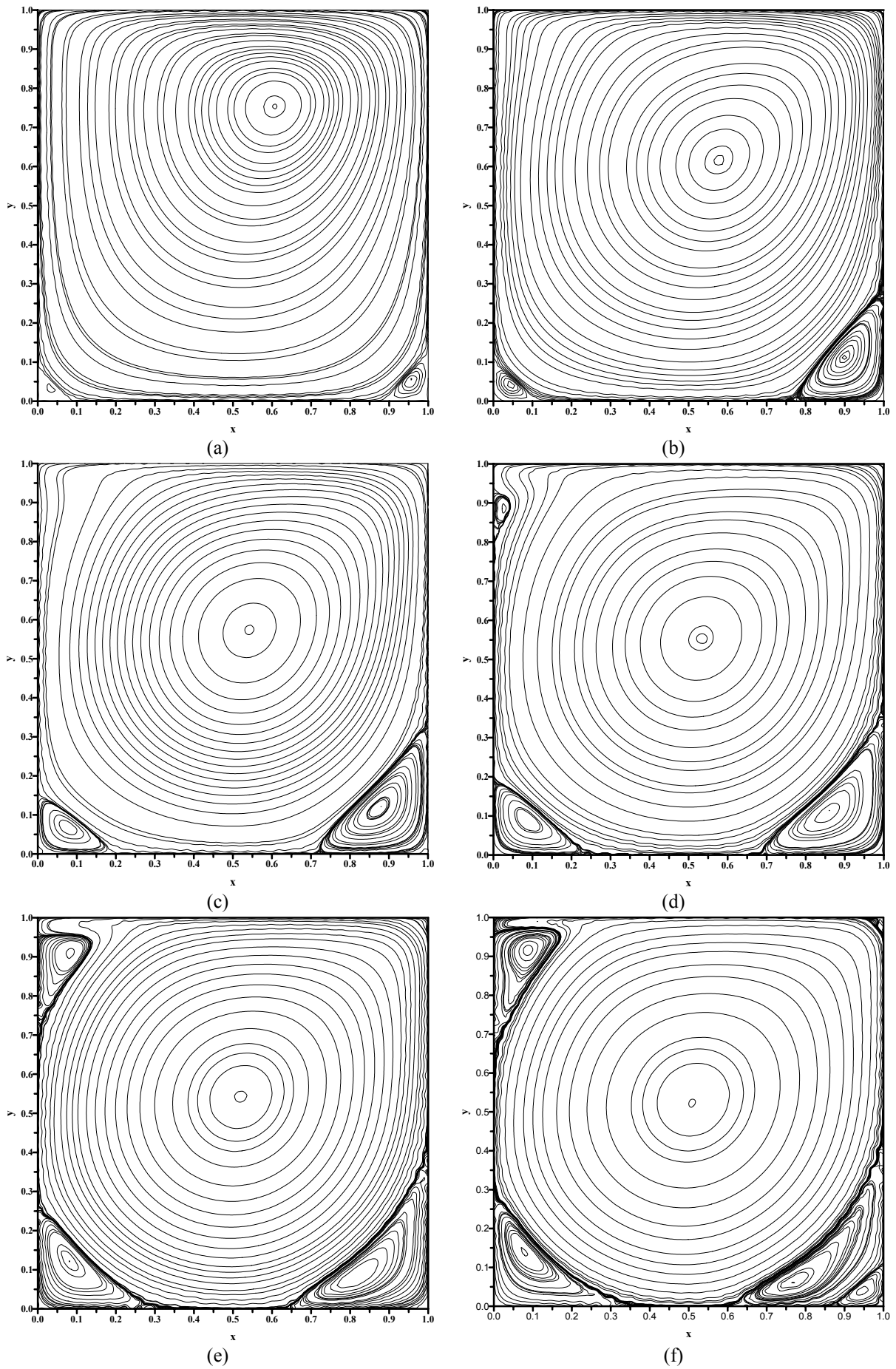
Figure 2. Streamlines for the regularized driven square cavity: (a) Re =100, (b) Re = 400, (c) Re = 1000, (d) Re = 2000, (e) Re = 5000, (f) Re = 10000.
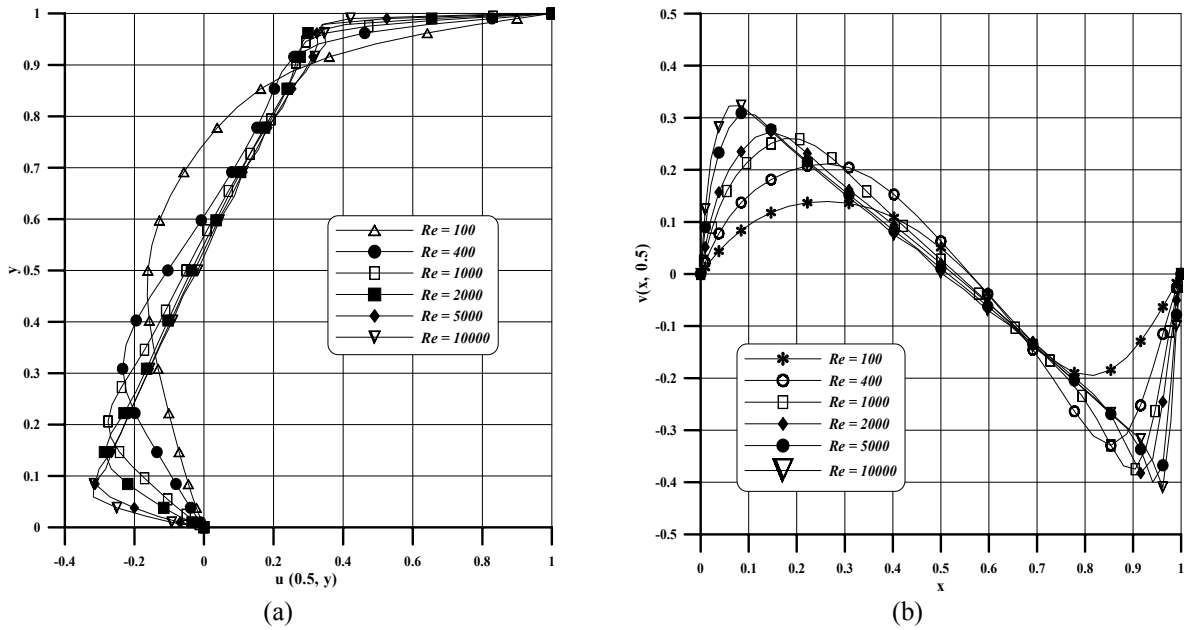
Figure 3. Variation of the velocity profile on the centerline for some Reynolds numbers: (a) u-velocity, (b) v-velocity.

4.2. Flow over a backward-facing step

The problem of steady viscous incompressible flow over a backward-facing step is a Benchmark problem that has been studied by numerous authors using a wide variety of numerical methods. Consider the area containing a step, as shown in Fig. 4, the channel is defined to have an unitary height H with a step height and localized in the upstream inlet region equally to $H/2$, the downstream channel length is $L = 30H$. The coordinates system to describe the locations in the channel is centered at the step corner. The definition of the problem as well as the nomenclature used are following Gartling (1990). The boundary conditions for the channel geometry are the no-slip conditions for all walls. The inlet velocity field is specified as a parallel flow with a parabolic horizontal component defined by $u(y) = 24y(0.5 - y)$ for $0 \le y \le 0.5$. This parabolic profile produces a maximum inflow velocity of $u_{max} = 1.5$ and an average inflow velocity $u_{avg} = 1.0$. The outflow boundary condition used is a velocity field obtained of parabolized Navier-Stokes incompressible equations and a buffer zone is placed in the end of the channel (see Fig. 4). The Reynolds number is defined by the relation $\mathbf{Re} = u_{avg}H/v$.
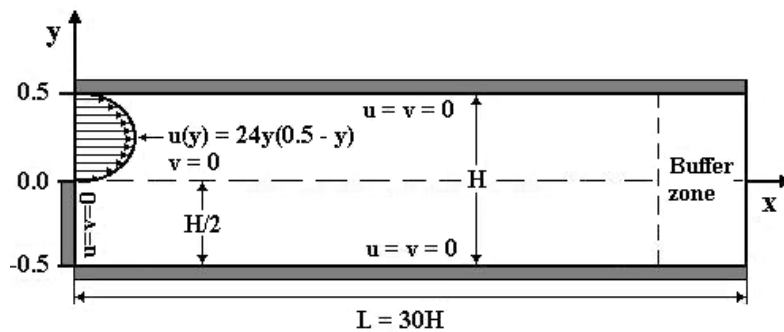
Figure 4. Geometry of the backward-facing step and boundary conditions.

A buffer zone technique (Streett & Macaraeg (1989/90)) is implemented on a single domain. This technique recognizes the fact that the source of possible reflections from the outflow boundary is in the elliptic nature of the Navier-Stokes equations arising from the viscous terms and the pressure field. The idea is remove this ellipticity at the outflow boundary. Then, the first source of ellipticity; the normal viscous terms are smoothly reduced to zero at the outflow boundary multiplying by a filter function s_j. Similarly, the ability of the pressure field to carry signals back into the domain from the outer boundary is attenuated to zero at outflow by multiplying the source term of the pressure Poisson equation by the filter function. In the present simulations, the filter function is expressed as

$$s_j = \frac{1}{2}\left(1 + \tanh\left\{4\left[1 - 2\frac{(j - N_b)}{(N_x - N_b)}\right]\right\}\right) \qquad (20)$$

where N_b is the number of the point than marks the begin of the buffer zone and N_x is the number of the point than marks the position of outflow boundary.

All numerical simulations for the backward-facing step flow were computed using a dimensionless channel length of **25H**, a grid of 91x61 points of Chebyshev collocations, the buffer zone was set on point 79 of the grid (using 12 point of collocation in this zone) and the time step used in all simulations was 0.001.

In the Figs. (5a)-(5d) can be observed the formation and growing of the vortices than appears at the top and bottom of the backward-facing step when the Reynolds number increases. These figures show mainly that the vortices for three Reynolds numbers (Re = 100, Re = 650, Re = 800 and Re = 875) can be very well represented using only 91x61 points of collocation.

(a)   (b)

(c)   (d)
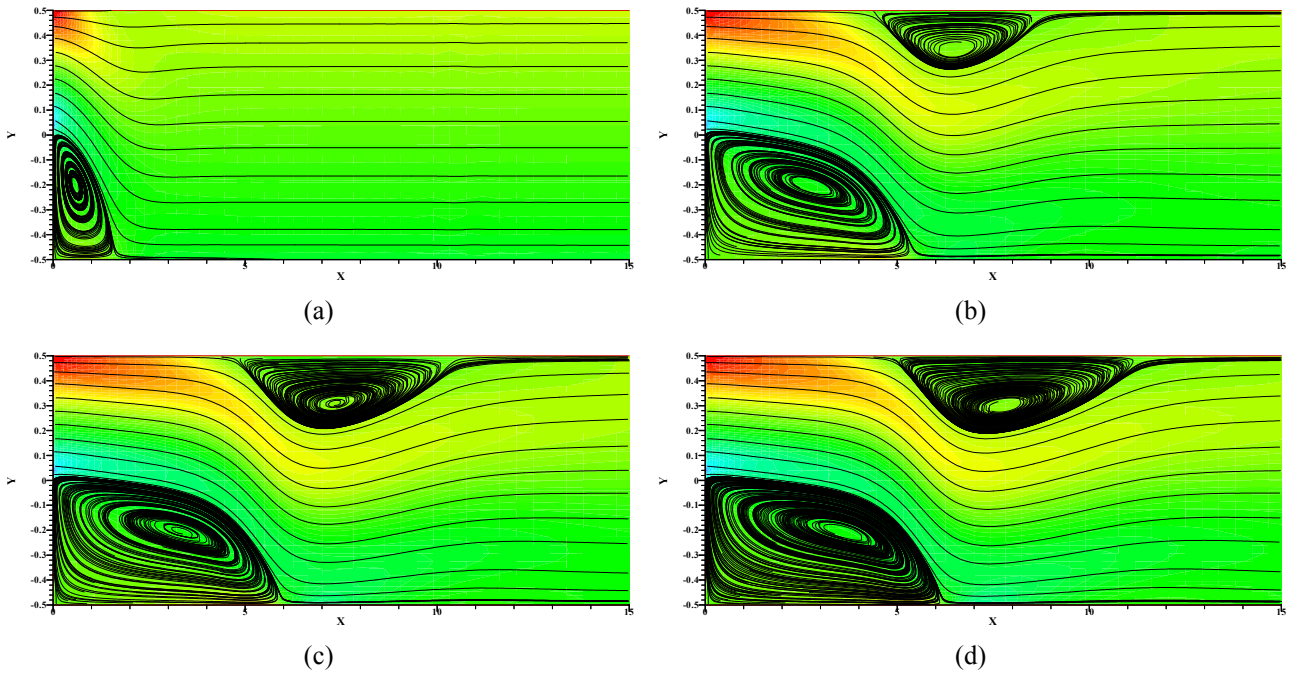
Figure 5. Steady-state streamlines of the backward-facing step: (a) Re = 100, (b) Re = 650, (c) Re = 800, (d) Re = 875.

The Tab. (2) shows the comparison of the some characteristic values of the backward-facing step for Re = 800 with previous numerical results obtained by Gartling (1990). Gartling (1990) used the finite element method with a grid of 400x40 elements. Although we have used only a grid of 91x61 points of Chebyshev collocation for all cases, the comparison of the positions of the separation and reattachments points are in good agreement with theirs.

Table 2. Comparison of some characteristic values of flow for Re = 800

Vortex	Localization (x,y)	Gartling (1990) Grid 400x40	Present method Grid 91x61
Top vortex	Separation point	(4.85, 0.50)	(4.81, 0.50)
	Reattachment point	(10.48, 0.50)	(10.45, 0.50)
Bottom vortex	Separation point	(0.00, 0.00)	(0.00, 0.00)
	Reattachment point	(6.10, 0.00)	(6.00, 0.00)

Finally, the Fig. (6a) show the comparison of *u* velocity profiles across the channel at x = 7 and x = 15 for Reynolds number of 800. Once again, can be observed the good agreement between velocity profiles obtained by the present method and the numerical velocity profiles obtained by Gartling (1990). The variation of *u* velocity profiles across the channel at x = 7 and x = 15 for a Reynolds number of 875 is shown in the Fig.(6b).
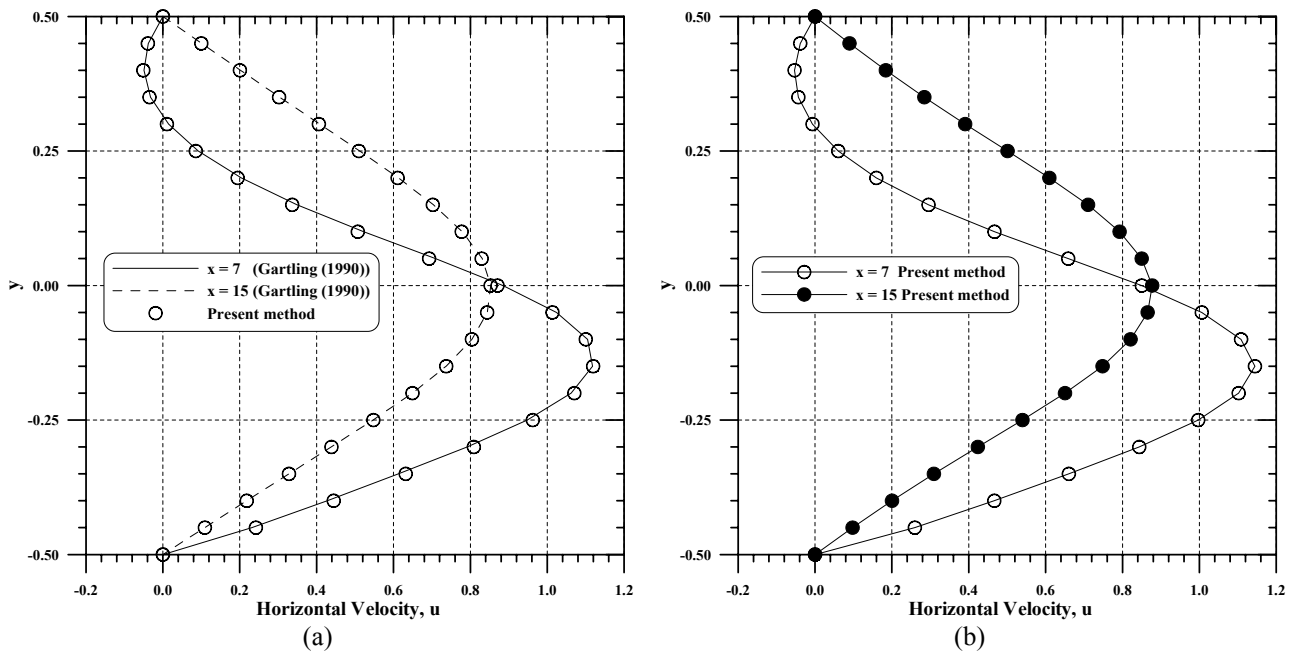
Figure 6. Comparison of u-velocity profiles across the channel at x = 7 and x = 15: (a) Re = 800, (b) Re = 875.

5. Conclusions

The projection method combined with the Chebyshev collocation spectral method associated with a second order explicit-implicit time scheme and appropriate boundary conditions, has shown to be a scheme very stable when applied to the solution of the incompressible Navier-Stokes equations.

This combination of the projection scheme in conjunction with a Chebyshev collocation spectral method has been able to predict very well the behaviors of the recirculating zones of the 2D regularized driven square cavity flow for Reynolds numbers up to 10000 and the separation zones of the steady viscous incompressible flow over a backward-facing step for Reynolds numbers up to 875. A good agreement was obtained from comparison of the numerical results obtained by the present method with available numerical solutions.

6. Acknowledgement

7. References

Boyd, J.P., 2001, "Chebyshev and Fourier Spectral Methods", Ed. Springer-Verlag, Berlin.
Brown, D.L., Cortez, R. and Minion, M.L., 2001, "Accurate projection methods for the incompressible navier-stokes equations", Journal of Computational Physics, Vol. 168, pp. 464-499.
Canuto, C., Hussaini, M., Quarteroni, A. and Zang, T.A., 1988, "Spectral Methods in Fluid Dynamics", Ed. Springer-Verlag, Berlin.
Chen, H., Su, Y. and Shizgal, B.D., 2000, "A direct spectral collocation poisson solver in polar and cylindrical coordinates", Journal of Computational Physics, Vol. 160, pp. 453-469.
Chorin, A. J., 1968, "Numerical solution of the navier-stokes equations", Mathematics of Computation, Vol. 22, pp. 745-762.
Gartling, D. K., 1990, "A test problem for outflow boundary conditions-Flow over a backward-facing step", International Journal for Numerical Methods in Fluids, Vol. 11, pp. 953-967.
Kim, J. and Moin, P., 1985, "Application of a fractional-step method to incompressible navier-stokes equations", Journal of Computational Physics, Vol. 59, pp. 308-323.
Shen, J., 1991, "Hopt bifurcation of the unsteady regularized driven cavity flow", Journal of Computational Physics, vol. 95, pp. 228-245.
Streett, C.L. and Macaraeg, M.G., 1989/90, "Spectral multi-domain for large-scale fluid dynamic simulations", Applied Numerical Mathematics, Vol. 6, pp. 123-139.
Tanahashi, T. and Okanaga, H., 1990, "GSMAC finite element method for unsteady incompressible navier-stokes equations at high Reynolds numbers", International Journal for Numerical Methods in Fluids, Vol.11, pp. 479-499.

Temam, R., 1968, "Une méthode d'approximation de la solution des équations de navier-stokes", Bulletin of Society Mathematics of France, Vol. 98, pp. 115-152.

8. Copyright Notice